Journal of Medicinal and Chemical Sciences 7 (2024) 1969-1981

Journal of Medicinal and Chemical Sciences

Journal homepage: http://www.jmchemsci.com/

Original Article

The Interaction of Isoniazid on 3D Structure Variation of NAT2 Gene and Its Effect on Drug Blood Levels

Dian Natasya Rahardjo[1,2], Yanuar Metriks Mutiara[3], Mariana Wahjudi[3,*], Retnosari Andrajati[1], Ratu Ayu Dewi Sartika[4]

[1] *Faculty of Pharmacy, Universitas Indonesia, Depok, Indonesia*
[2] *Faculty of Pharmacy, University of Surabaya, Surabaya, Indonesia*
[3] *Master of Biotechnology, University of Surabaya, Surabaya, Indonesia*
[4] *Faculty of Public Health, Universitas Indonesia, Depok, Indonesia*

ARTICLE INFO

Article history

Received: 2024-11-12
Received in revised: 2024-11-21
Accepted: 2024-12-11
Manuscript ID: JMCS-2411-2676

DOI:10.26655/JMCHEMSCI.2024.12.15

KEYWORDS

N-acetyltransferase 2
Isoniazid
Tuberculosis
Polymorphism
Acetylator
Molecular docking

ABSTRACT

Drug-Resistant Tuberculosis (DR-TB) and Anti-TB Drug-Induced Liver Injury (AT-DILI) are frequently linked to polymorphisms in drug-metabolizing enzymes (DMEs). Among these, arylamine N-acetyltransferase 2 (NAT2) plays a pivotal role in metabolizing isoniazid (INH). This study investigates the structural and functional effects of NAT2 polymorphisms on INH interactions. Using the 3D structure of wild-type NAT2 (PDB ID: 2PFR) as a template, we employed Chimera, AutoDock, GROMACS, and VMD software for molecular docking and dynamic simulations. Five common coding SNPs in NAT2—G191A, T341C, G590A, A803G, and G857A—were combined to produce 15 mutant NAT2 variants. The DNA sequences of 12 TB patients from a public health center in Surabaya, Indonesia, were used to correlate acetylator phenotypes with the INH blood levels. The molecular docking analysis revealed that the binding affinity of INH to wild-type NAT2 was -5.7 kcal/mol, which is similar to most mutants. Minor variations were observed among the mutants, with affinities ranging from -5.6 to -5.7 kcal/mol. Mutants 2, 6, 8, 9, 10, 12, 14, and 15 (rapid acetylators) showed a decrease in interaction with residue G124, while new binding with residue L288 was identified in mutants 1, 3, 4, 5, and 7 (slow acetylators). These discrepancies in interactions point to a structural foundation for disparities in acetylation rates and enzyme activity. Correlations between the INH–NAT2 interaction patterns and patient acetylator phenotypes revealed distinct impacts on INH blood levels, highlighting potential implications for DR-TB treatment outcomes and AT-DILI risk.

* Corresponding author: Mariana Wahjudi
✉ E-mail: mariana_wahyudi@staff.ubaya.ac.id

GRAPHICAL ABSTRACT

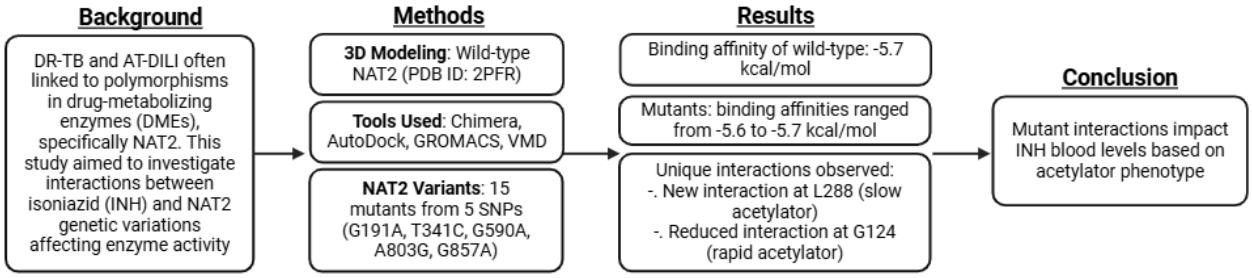

Introduction

Mycobacterium tuberculosis is estimated to have infected a quarter of the world's population, causing several asymptomatic cases of Tuberculosis (TB) and latent TB infection (LTBI) [1]. In 2022, the global distribution of TB shows that approximately 46% of cases occur in the Asian region, with Indonesia ranking second as the country with the highest number of patients in the world. Based on data from *tbindonesia.or.id*, the success rate of TB treatment in Indonesia is 86%, indicating that 14% of patients experience therapy failure. Moreover, the occurrence of drug-resistant TB (DR-TB) and therapy failure is often attributed to low drug blood levels [2,3].

Drug metabolizing enzymes (DMEs) polymorphism can affect the achievement of a therapeutic range of drug blood levels in TB patients. Isoniazid (INH) is one of the first-line anti-TB drugs. INH will be acetylated by NAT2 protein into acetylisoniazid, hydrolyzed into acetylhydrazine, and re-acetylated by NAT2 into non-toxic diacetylhydrazine. Acetylhydrazine can also be produced from the hydrolysis process of INH into hydrazine, which passes through acetylation into acetylhydrazine. Moreover, an acetylhydrazine compound that has been proven to be hepatotoxic in animals is monoacetylhydrazine. This compound is oxidized by cytochrome P450 CYP2E1 to produce other compounds that have the potential to be hepatotoxic, such as acetyldiazene, ketene, or acetylonium ions [4-7].

In several studies on NAT2 polymorphism, patients can be classified into three phenotypic groups, namely rapid, intermediate, and slow acetylator phenotypes. The patients with NAT2 slow acetylator phenotype might have high levels of INH in the body because INH is metabolized slower. It can increase the harm risk of anti-TB drug-induced liver injury (AT-DILI). However, those with rapid acetylator phenotype NAT2 gene are at high risk of developing DR-TB. This is because INH is rapidly metabolized to form diacetylhydrazine, preventing drug concentration from reaching the therapeutic range and causing ineffective treatment [8]. Rapid acetylator phenotype is commonly found in DR-TB patients, while slow acetylator phenotype is often observed among AT-DILI patients. NAT2 gene is located on the short arm of chromosome 8 (8p21.3-23.1) and contains 870 bp. The most common allele in Asia is NAT2*4, while NAT2*5 is found in Caucasians and Africans. The frequency of slow acetylator phenotype in Asia is 5-30% and 40-90% in African and Caucasian populations. Although the genotype-phenotype relationship in NAT2 has been widely studied, the precise correlation has not been clearly explained. Several studies have shown a high level of agreement between genotype and phenotype, but there is no 100% correlation. The genotypes NAT2*4, NAT2*12A, and NAT2*13 are associated with the rapid acetylator phenotype, while NAT2*5, NAT2*6, and NAT2*7 are correlated with the slow acetylator phenotype [9].

Due to the absence of a precise relationship, an in-silico study on the interaction of INH with variations in the 3D structure of the NAT2 gene is needed to show the correlation between INH and the NAT2 gene. This interaction must be supported by clinical data showing that differences in NAT2 genotype types are related to the achievement of INH levels in the blood. Furthermore, an in silico study should focus on the NAT2*6A allele, which is prevalent in Indonesia, particularly among the Javanese population, with a percentage of 36.8% and is widely recognized as a slow acetylator phenotype [9].

Given the critical role of NAT2 in metabolizing isoniazid (INH) and its potential contribution to drug resistant tuberculosis (DR-TB) and anti-TB drug-induced liver injury (AT-DILI), this study investigates the structural and functional impact of NAT2 polymorphisms on INH metabolism. Using a combination of molecular docking and patient-derived data, this study aims to: (1) evaluate the binding interactions between INH and wild-type/mutant NAT2 genotypes, (2) identify structural changes that influence these interactions, and (3) correlate these findings with NAT2 acetylator phenotypes and INH blood levels in a cohort of TB patients. This integrated approach provides new insights into the molecular basis of NAT2 variability and its implications for personalized TB therapy [9].

Method

The Human NAT2 Sequence Variants

The sequences of human NAT2 variants were accessed from the National Center for Biotechnology Information (NCBI) database. The NAT2 protein reference had an accession number of P11245_2 or NP_000006.2. The database recorded more than nineteen polymorphic sites. In this study, we studied several haplotypes of five SNPs because these alleles were commonly found. The sequences of NAT2 chosen allele variants are listed in Table 1.

Building of the 3D Structure of NAT2 Variants Protein and INH

The 3D structure of each haplotype was built by a Swiss-model modeling tool with 2pfr.1.A structure as a model template. In addition, the 3D structure was built using another tool at RCSB-PDB (https://www.rcsb.org/). Furthermore, 15 mutation variations 3D structures were carried out by replacing amino acid residue at the polymorphic site based on the protein sequence of P11245_2 (Table 1) using Chimera 1.14 software. Energy minimization was performed on the mutant structure to obtain 3D conformation in a normal state in pdb format using the YASARA web server (http://www.yasara.org/servers.htm). This process produced a 3D structure of the mutant receptor, which was ready for docking preparation. The 3D structure of the INH ligand was obtained from the PubChem database (PubChem CID: 3767) (https://pubchem.ncbi.nlm.nih.gov/) in sdf format, which was converted into pdb format using Marvin View software.

Table 1: NAT2 variants and residue substitutions

Variation Number	Number of SNP' site	Residue Substitution
1	1	G286R (Glycine to Arginine at position 286)
2	1	K268R (Lysine to Arginine at position 268)
3	1	R197Q (Arginine to Glutamine at position 197)
4	1	I114T (Isoleucine to Threonine at position 114)
5	1	R64Q (Arginine to Glutamine at position 64)
6	5	R64Q, I114T, R197Q, K268R, and G286R
7	2	K268R G286R
8	2	R197Q and K268R
9	2	I114T and R197Q
10	2	R64Q and I114T
11	3	R197Q, K268R, and G286R
12	3	I114T, R197Q, and K268R
13	3	R64Q, I114T, and R197Q
14	4	I114T, R197Q, K268R, and G286R
15	4	R64Q, I114T, R197Q, and K268R

Validation, Molecular Docking, and Molecular Dynamics

Validation was performed with a 3D structure of NAT2 as wild-type (PDB ID: 2PFR). The grid box was considered valid when the binding pattern

was similar to the reference ligand, with Root Mean Square Deviation (RMSD) below 2 Armstrong, and binding to the active site residues. Molecular docking was performed using Autodock Vina with INH as a ligand, while wild-type NAT2 and mutants served as receptors at standard settings. Subsequently, molecular dynamics were performed using GROMACS with the 3rd mutant complex (NAT2*6B) as an object with 100 mM NaCl settings at 37 °C, 1 atm.

Visualization of Molecular Docking and Molecular Dynamic Results

2D visualization was performed using LigPlus to determine the NAT2-INH binding pattern. Furthermore, 3D visualization of molecular docking and molecular dynamic results was performed using VMD.

Prediction of Acetylator Phenotype in TB Patients

Blood samples were obtained from 12 new TB patients at a Public Health Center in Surabaya City. The sampling procedure in TB patients has followed ethical standards and obtained approval from the institutional ethics committee. Each patient in this study has received detailed information and has signed an informed consent. Genomic DNA sample extraction was performed using the TIANamp Genomic DNA Kit from Tiangen.

Subsequently, DNA sequencing was performed using nanopore technology with the MinION Mk1B device - Oxford Nanopore Technologies®. Analysis of the nucleotide sequence and NAT2 allele variations was carried out using the "EPI2ME" application. The allele obtained was used to predict the acetylator phenotype, which was guided by the database https://nat.mbg.duth.gr.

Determination of INH Blood Levels

Blood sampling was carried out 2 hours after patients took oral antituberculosis medication (OAT). Determination of blood levels was performed using an HPLC-MS/MS (high-performance liquid chromatography/tandem mass spectrometry) instrument. A total of 3 ml blood specimens were centrifuged at 3000 rpm, followed by the collection of serum for further processing.

Simple extraction was carried out using protein precipitation with 150 µL of 15% trichloroacetic acid in 300 µL of serum. This mixture was vortexed for 2 minutes and centrifuged at 3000 rpm for 10 minutes. Subsequently, the supernatant was collected, and 20 µL was injected into the HPLC. The stationary phase used was a Novapak® C18 Column (150 x 3.9 mm, 3 microns). The mobile phase consisted of 0.05 M sodium dihydrogen phosphate and acetonitrile (97:3) with a flow rate of 1 mL/min at room temperature, with detection being carried out at λ 280 nm.

Results

3D Structure of Human NAT2 and INH

In exon 2, there are 7 SNPs, but only 5 cause protein variations, including those at positions 191, 341, 590, 803, and 857. These variations led to a wide range of receptors, comprising 15 mutants and 1 wild-type. In addition, a 3D structure of INH was obtained (PubChem CID: 3767) for further analysis.

Validation, Molecular Docking, and Molecular Dynamics

A comparison visualization of the binding pattern was carried out between the reference and ligand, which resulted from docking. The result showed that both ligands had similar patterns, with RMSD below 2 Armstrong, binding to the active site residues; thereby, the grid box was considered valid, as displayed in Figure 1.

After validation, molecular docking was carried out between INH and NAT2. The results showed good interaction from the binding affinity values, as presented in Table 2.

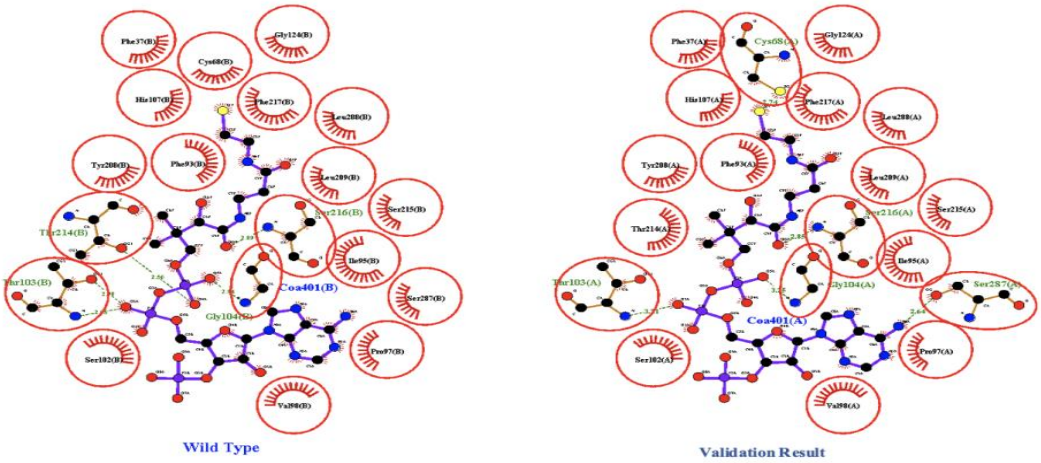

Figure 1: Analysis of wild-type CoA ligand binding pattern and validation results with 2D visualization

Table 2: Binding affinity of INH interaction with various receptors

Receptor	*Binding affinity* (kcal/mol)	Mutants with Similar Behavior
Wild-type	-5.7	--
Mutants (Group 1)	-5.7	1, 2, 3, 4, 5, 7, 8, 9, 11, 13, 14, 15
Mutants (Group 2)	-5.6	6, 10, 12

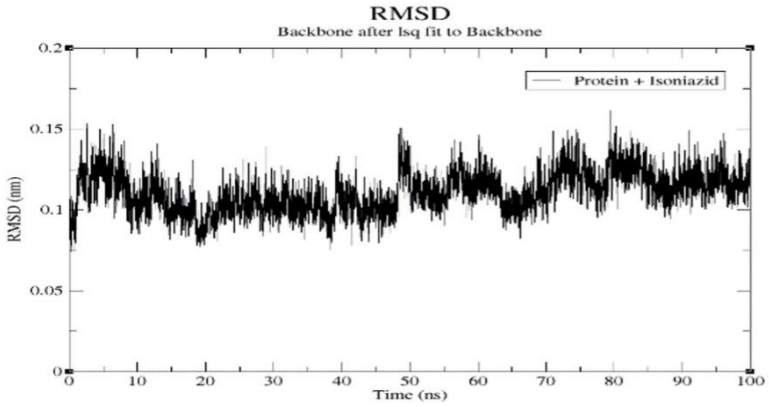

Figure 2: Interpretation of RMSD of molecular dynamic results

Based on the molecular dynamic simulation presented in Figure 2, the RMSD value of NAT2 mutant 4 with INH was obtained as 0.11 nm (1.1 Å). RMSD is a comparison between 2 predicted pose values, with smaller RMSD indicating more valid predicted interaction between receptor and ligand. The flexibility of NAT2*6B (mutant 3) - INH complex can be analyzed from molecular dynamic simulations using the Root Mean Square Fluctuation (RMSF) parameter, as shown in Figure 3. Moreover, greater residue fluctuation shows higher flexibility in the treatment during simulation [10].

Visualization of Molecular Docking and Molecular Dynamic Results

The results of 2D visualization of the molecular docking using LigPlus showed the formation of hydrophobic and hydrogen bonds between the ligand and the receptor protein residues. Furthermore, mutant 1 has the same bonding pattern as mutants 3, 4, 5, and 7. Mutant 2 has the same bonding pattern as mutants 6, 8, 9, 10, 12, 14, and 15. Wild-type has the same bonding pattern as mutants 11 and 13. 3D visualization presented in Table 3 shows the interaction of ligands with residues on the receptor.

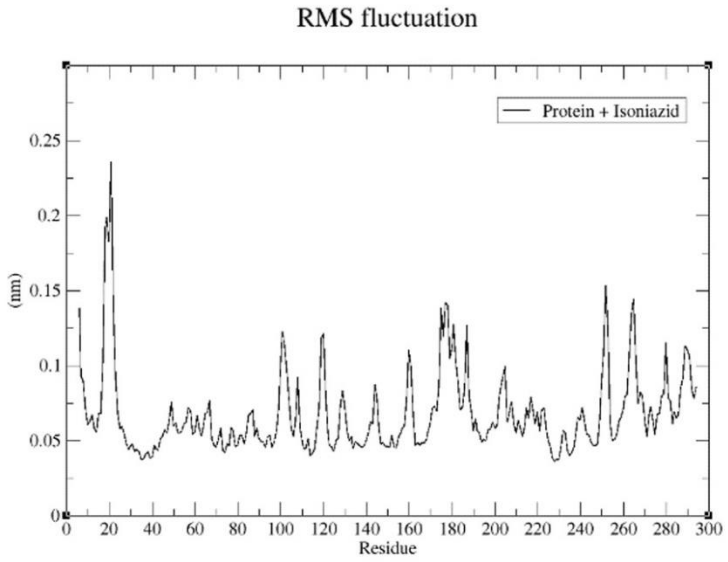

Figure 3: Interpretation of RMSF results from molecular dynamics

Table 3: 2D and 3D visualization of INH interactions with various receptors

Receptor Variant	2D Visualization	3D Visualization
Wild-type	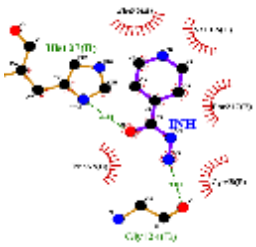	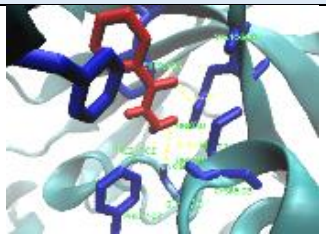
Variant Receptor No.	**2D Visualization**	**3D Visualization**
1	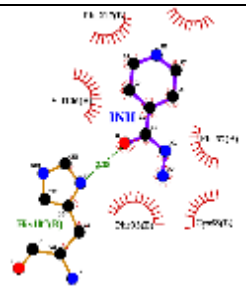	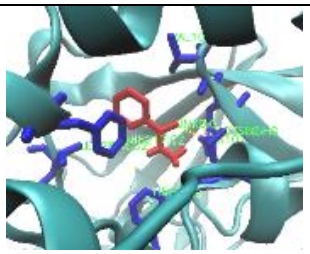
2	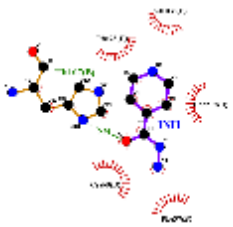	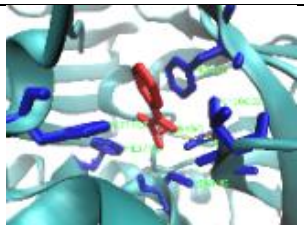
3	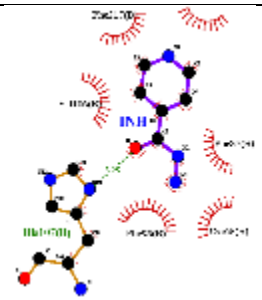	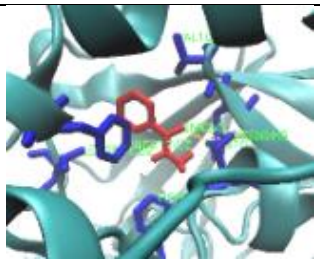

Receptor Variant	2D Visualization	3D Visualization
4	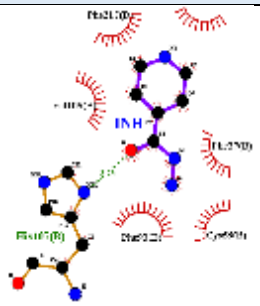	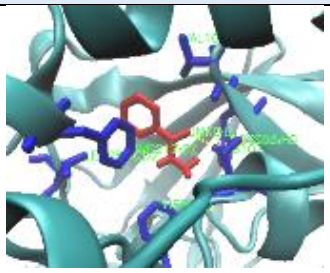
5	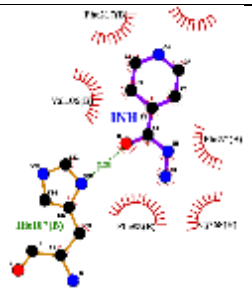	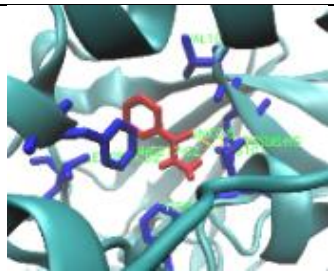
6	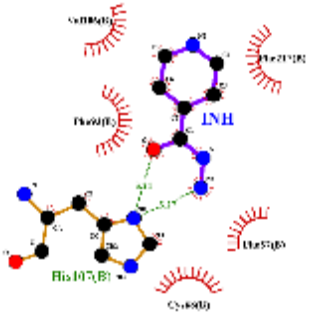	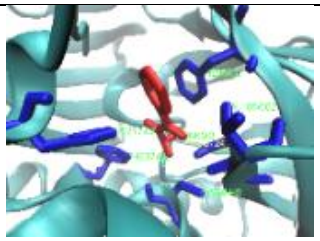
7	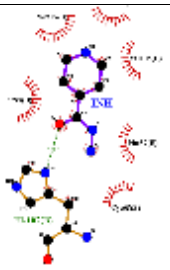	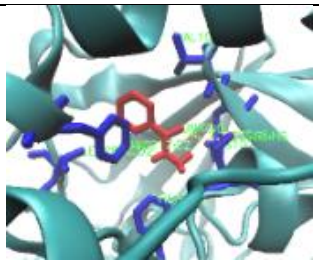
8	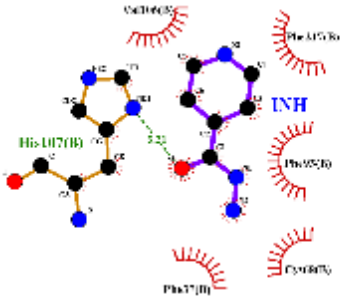	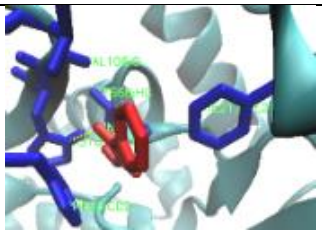
9	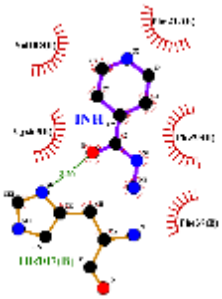	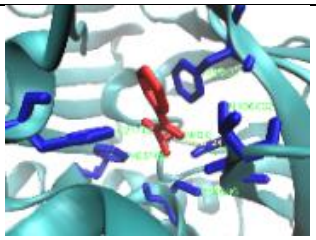

Receptor Variant	2D Visualization	3D Visualization
10	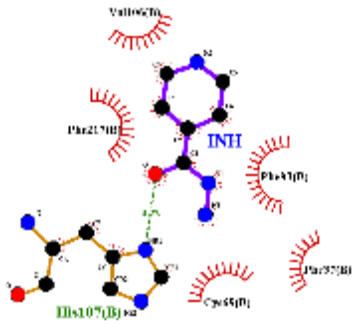	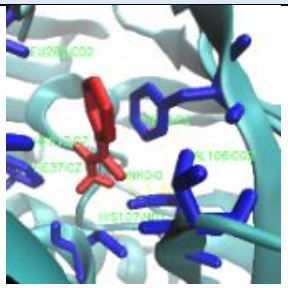
11	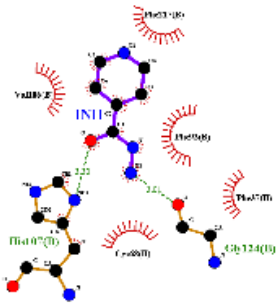	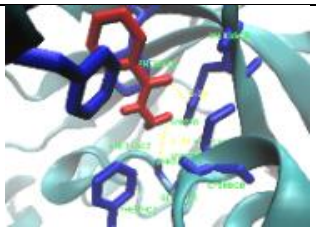
12	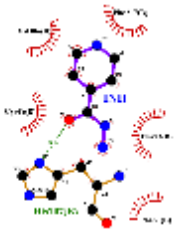	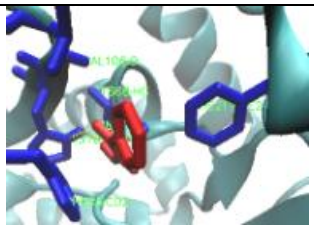
13	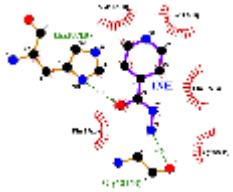	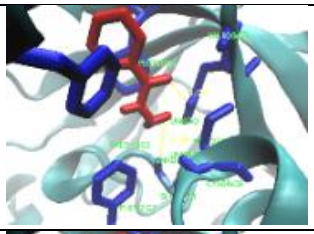
14	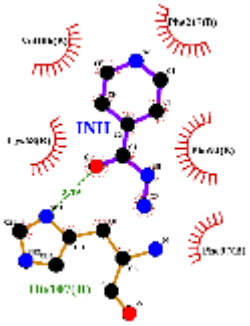	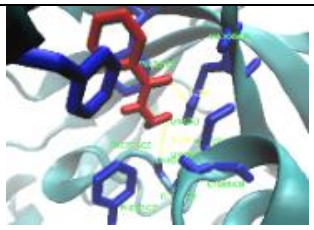
15	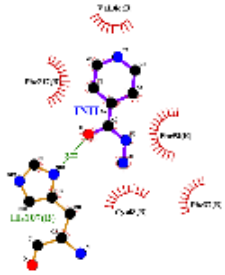	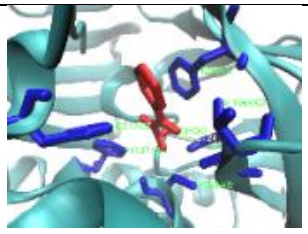

n receptor n hydrogen bond
n interacting residues n residue label
n ligand

Table 4: Association between acetylator phenotype and INH blood levels

Acetylator phenotype	INH levels (µg/ml) Mean ± SD (Min-Max)	*P*-value
Rapid	1.146 ± 0.4494 (0.45 – 1.57)	0.0389*
Slow	1.783 ± 0.0551 (1.73 – 1.84)	

** = p < 0.05 (Unpaired t-test)*

Association between Acetylator Phenotype and INH Blood Levels

Based on the polymorphism examination conducted on 12 blood samples, a total of 9 patients were found with rapid acetylator phenotype, while 3 had slow acetylator phenotype. The results showed that there were differences in INH levels in the blood between patients with rapid and slow acetylator phenotypes, as provided in Table 4.

Discussion

The visualization of INH ligand interaction with NAT2 receptor variations showed a strong correlation. This was evidenced by the presence of hydrophobic and hydrogen bonds between INH and the receptor protein residues, along with a negative binding affinity value. The pose of a ligand is considered close to the native and valid stated when the RMSD value is below 2Å. In this study, binding affinity value of INH-NAT2 wild-type interaction is -5.7 kcal/mol and INH-NAT2 mutant variations 1 to 15 are sequentially -5.7, -5.7, -5.7, -5.7, -5.7, -5.6 -5.7, -5.7, -5.7, -5.6 -5.7, -5.6, -5.7, -5.7, and -5.7 kcal/mol. INH ligand bound to wild-type NAT2 forms hydrogen bonds with residues H107 and G124 and hydrophobic bonds with residues C68, F37, F217, V106, and F93. The C68 residue in NAT2 plays an important role in the enzymatic activity, serving as a recipient of the donor acetyl group from acetyl-CoA to be transferred to the substrate, namely INH [11]. In this study, mutations were carried out on 15 variations of SNPs coding combinations to determine the effect on receptor binding to ligands. The analysis was based on a previous study indicating that changes in the structure of enzymes led to variations in the selectivity and working ability [12]. The results of LigPlus analysis, comparing the binding patterns, showed that mutants 11 (R197G K268R G286R) and 13 (R64Q I114T R197Q) did not experience changes. The binding pattern in these mutants was the same as with wild-type structures, both in hydrogen and hydrophobic bonds, showing an insignificant effect on ligand binding [13]. This could be attributed to the structural changes due to the formation of SNPs that support ligand binding perfectly to the catalytic residue. Mutant 1 (G286R) experienced a change in binding pattern, namely the loss of interaction with residue G124 and the formation with L288. However, hydrogen bonds with residues H107 and F93, as well as hydrophobic bonds with V106, F37, C68, and F217, were unaffected. The same change in the binding pattern also occurred in mutants 3 (R197Q), 4 (I114T), 5 (R64Q), and 7 (L268R G286R). G286R SNP produced the NAT2*7A allele, which had a slow acetylator phenotype. This suggested that the loss of interaction with residue G124 and the formation with L288 affected the 3D conformation of NAT2, thereby reducing the activity in the catalysis of INH metabolism. Based on the data from the SNPedia database, SNPs in mutants 3, 4, and 5 would form NAT2 with a slow acetylator phenotype, namely NAT2*6B, NAT2*5A, and NAT2*14A alleles. Additional interactions with the L288 residue could cause shifts in amino acid residues around the active site, preventing the enzyme-substrate interaction from entering perfectly at the binding site [14]. This was in line with the results of a previous study on three patients with a slow acetylator phenotype, who achieved higher blood INH levels compared to patients with a rapid acetylator phenotype. Changes in binding pattern were found in mutant 2 (L268R), namely the loss of hydrogen bond interaction with G124 residue. Furthermore, there were changes in binding

pattern of mutants 6 (R64Q I114T R197Q L268R G286R), 8 (L268R G286R), 9 (I114T R197Q), 10 (R64Q I114T), 12 (I114T R197Q L268R), 14 (I114T R197Q L268R G286R), and 15 (R64Q I114T R197Q L268R). These data suggested that the loss of interaction with G124 residue changed the 3D conformation of NAT2, causing an increase in catalytic activity. As supported by NAT2*12A, mutant 2 was listed in the SNPedia database as a rapid phenotype NAT2 allele. The loss of interaction with G124 residue caused a shift in the amino acid residues around the active site that prevented the cofactor or substrate from entering perfectly at the binding site [15]. The increased NAT2 enzyme activity correlated with the results of INH levels in the blood of 9 patients with a rapid phenotype.

In this study, the interaction of wild-type NAT2-INH formed hydrogen bonds with residues H107 and G124, as well as hydrophobic bonds with residues C68, F37, F217, V106, and F93. Specifically, mutant 2 (K268R) formed hydrogen bonds with residue H107 and hydrophobic bonds with residues C68, F37, F217, V106, and F93. Unissa (2017) reported that the interaction of wild-type NAT2-INH correlated with residues G124, F37, S125, G126, S127, C68, L288, F93, L209, V106, F217, and H107 [16]. The K268R-INH mutant NAT2 formed interactions with L288, S216, F217, F37, S125, G124, F93, H107, C68, and V106. The results were inversely proportional compared to the previous study, as evidenced by the formation of interaction with G124 residue. This difference was attributed to the use of the 3D structure of wild-type Homo sapiens NAT2 (PDB ID: 2PFR) as a reference, while the previous study applied Mycolicibacterium smegmatis NAT (PDB ID: 1W6F).

A molecular dynamic simulation was carried out on the NAT2*6B mutant as a method for the NAT2*6A allele to determine the stability during interaction with INH. NAT2*6A allele was found to be the most dominant in Indonesia, with a percentage of 36.8% [9]. The results of the molecular dynamic visualization showed RMSD value for the mutant receptor 3 with INH of 0.11 nm (1.1 Å) and a fairly fluctuating RMSF. The analysis showed that after simulation, the NAT2 enzyme structure was unable to survive, indicating instability at ambient temperatures. However, the results of the molecular dynamics simulation were significantly representative of the existing theory, showing that INH was moving from the receptor.

Limitation

One of the limitations of this study is the relatively small sample size (n=12), which may reduce the generalizability of the findings. The limited number of participants, recruited from a single public health center, could introduce sampling bias and may not fully represent the genetic diversity of the larger population. Furthermore, the small sample size limits the statistical power to detect subtle variations in INH blood levels across different acetylator phenotypes. While the molecular docking results are consistent across wild-type and mutant NAT2 genotypes, the biological validation of these interactions would benefit from a larger cohort to confirm these patterns. Future studies should aim to include a broader and more diverse participant pool to enhance the robustness and applicability of the findings.

In addition, the relationship between NAT2 polymorphisms, acetylation phenotypes, and INH pharmacokinetics may be influenced by other genetic and environmental factors not accounted for in this study. Expanding the sample size and incorporating multivariate analyses would provide a more comprehensive understanding of these complex interactions.

Conclusion

This study demonstrates that variations in the NAT2 genotype, particularly the mutations affecting residues G124 and L288, may influence the phenotypic outcomes of INH metabolism, potentially leading to differing acetylator profiles in patients. While these results highlight a correlation between specific mutant combinations and altered binding interactions with INH, the relationship between these molecular changes and clinical treatment outcomes requires further investigation.

In terms of treatment implications, the findings suggest that adjusting the INH dose based on the acetylator phenotype could enhance therapeutic efficacy and minimize adverse drug reactions. Specifically, patients with slow acetylator phenotypes (such as those associated with the first mutant group) might benefit from higher INH doses, while individuals with rapid acetylator phenotypes (e.g., the second and third mutant groups) may require lower doses to avoid toxicity. However, these recommendations should be contextualized by individual patient factors such as age, weight, gender, comorbidities, and potential drug-drug interactions—variables that were not considered in this study.

This study represents the first step in identifying the roles of residues G124 and L288 in influencing the activity of NAT2 and the resultant acetylator phenotypes. Moving forward, clinical studies with larger sample sizes are needed to validate these findings and explore the direct impact of these mutations on INH pharmacokinetics. Moreover, further *in silico* analyses combined with experimental enzymatic assays could provide deeper insights into the mechanistic underpinnings of NAT2 activity and its role in drug resistance and liver injury.

Acknowledgments

Funding for this project was provided by World Class Research Grant 2021, Kementerian Pendidikan, Kebudayaan, Riset, dan Teknologi Republik Indonesia, 003 /AMD-SP2H/LT-MULTI-PDPK/LL7/2021,028/SP-Lit/AMD/LPPM-01/Dikbudristek/Multi/FTB/VII/2021. The authors would like to express their sincere gratitude to Laurentius Ivan Tedjokusumo and Viviana Arwanto for their invaluable technical assistance throughout this research project.

Authors' Contributions

Concept – D.N.R, M.W; Design – D.N.R, Y.M.M, and M.W; Supervision – D.N.R, M.W, and R.A; Resources – D.N.R, M.W; Materials – D.N.R, Y.M.M, and R.A.; Data Collection and/or Processing – D.N.R, Y.M.M, R.A., and R.A.D.S.; Analysis and/or Interpretation – D.N.R, Y.M.M, R.A., and R.A.D.S.; Literature Search – D.N.R, R.A., and R.A.D.S..; Writing – D.N.R, Y.M.M, and M.W.; Critical Reviews – D.N.R, Y.M.M, M.W, R.A., and R.A.D.S..

Disclosure Statement

The authors declared no conflict of interest in the study.

Ethical Clearance

This study has been reviewed and approved by the Institutional Ethics Committee of the University of Surabaya with No.223/KE/XII/2022.

ORCID

Dian Natasya Rahardjo
https://orcid.org/0000-0002-9634-6983
Yanuar Metriks Mutiara
https://orcid.org/0009-0000-3808-2046
Mariana Wahjudi
https://orcid.org/0000-0002-5861-2566
Retnosari Andrajati
https://orcid.org/0000-0003-1319-1240
Ratu Ayu Dewi Sartika
https://orcid.org/0000-0001-5018-7625

References

[1]. a) Mostafa H.K., Risan M.H., Al Faham M., A study of Mycobacterium tuberculosis Zopf, 1883 (Mycobacteriaceae) in Iraq, *International Journal of Advanced Biological and Biomedical Research*, 2022, **10**:1 [Crossref], [Google Scholar], [Publisher] b) Sterling T.R., Guidelines for the treatment of latent tuberculosis infection: recommendations from the National Tuberculosis Controllers Association and CDC, 2020, *MMWR. Recommendations and Reports*, 2020, **69** [Crossref], [Google Scholar], [Publisher]

[2]. a) Ayoubi S., Hashemzadeh M.S., Azar O.L., Naeimpour F., Padasht N., Mirtajani B., Aghajani J., Tat M., Sharti M., Dorostkar R., CASRP Publisher, Relationship between the human T- lymphotropic virus and myeloid leukemia, mycobacterium tuberculosis, *International Journal of Advanced Biological and Biomedical Research*, 2016, **4**:152 [Crossref], [Google Scholar], [Publisher] b) Lei Q., Wang H., Zhao Y., Dang L., Zhu C., Lv X., Wang H., Zhou J., Determinants of serum concentration of

first-line anti-tuberculosis drugs from China, *Medicine*, 2019, **98**:e17523 [Crossref], [Google Scholar], [Publisher]
[3]. Park J.S., Lee J.Y., Lee Y.J., Kim S.J., Cho Y.J., Yoon H.I., Lee C.T., Song J., Lee J.H., Serum levels of antituberculosis drugs and their effect on tuberculosis treatment outcome, *Antimicrobial Agents and Chemotherapy*, 2016, **60**:92 [Crossref], [Google Scholar], [Publisher]
[4]. Huang Y.S., Recent progress in genetic variation and risk of antituberculosis drug-induced liver injury, *Journal of the Chinese Medical Association*, 2014, **77**:169 [Crossref], [Google Scholar], [Publisher]
[5]. Perwitasari D.A., Atthobari J., Wilffert B., Pharmacogenetics of isoniazid-induced hepatotoxicity, *Drug metabolism reviews*, 2015, **47**:222 [Crossref], [Google Scholar], [Publisher]
[6]. Wahyudi A.D., Soedarsono S., Farmakogenomik hepatotoksisitas obat anti tuberkulosis, *Jurnal Respirasi*, 2019, **1**:103 [Crossref], [Publisher]
[7]. Erwin E.R., Addison A.P., John S.F., Olaleye O.A., Rosell R.C., Pharmacokinetics of isoniazid: The good, the bad, and the alternatives, *Tuberculosis*, 2019, **116**:S66 [Crossref], [Google Scholar], [Publisher]
[8]. a) Yousefi R., Molecular docking study of rosmarinic acid and its analog compounds on sickle cell hemoglobin, *Eurasian Journal of Science and Technology*, 2024, **4**:303 [Crossref], [Google Scholar], [Publisher] b) Hein D.W., Millner L.M., Arylamine N-acetyltransferase acetylation polymorphisms: paradigm for pharmacogenomic-guided therapy-a focused review, *Expert Opinion on Drug Metabolism & Toxicology*, 2021, **17**:9 [Crossref], [Google Scholar], [Publisher]
[9]. a) Suborna S.A., Lubna F.I., Hasan M.H., Ibnul I., Is the Amino Acid HIS458 and ASP/ASN206 of Laccase from T. versicolor and T. hirsuta crucial for the decolorization of polycyclic aromatic textile dyes? An in silico investigation, *Eurasian Journal of Science and Technology*, 2025, **5**:[Crossref], [Google Scholar], [Publisher] b) Yuliwulandari R., Sachrowardi Q., Nakajima H., Kashiwase K., Hirayasu K., Mabuchi A., Sofro A.S.M., Tokunaga K., Association of HLA-A,-B, and-DRB1 with pulmonary tuberculosis in western Javanese Indonesia, *Human Immunology*, 2010, **71**:697 [Crossref], [Google Scholar], [Publisher]
[10]. Huang Y., Zhang X., Suo H., Interaction between β-lactoglobulin and EGCG under high-pressure by molecular dynamics simulation, *PloS One*, 2021, **16**:e0255866 [Crossref], [Google Scholar], [Publisher]
[11]. Zhang N., Liu L., Liu F., Wagner C.R., Hanna P.E., Walters K.J., NMR-based model reveals the structural determinants of mammalian arylamine N-acetyltransferase substrate specificity, *Journal of Molecular Biology*, 2006, **363**:188 [Crossref], [Google Scholar], [Publisher]
[12]. Song Z., Zhang Q., Wu W., Pu Z., Yu H., Rational design of enzyme activity and enantioselectivity, *Frontiers in Bioengineering and Biotechnology*, 2023, **11**:1129149 [Crossref], [Google Scholar], [Publisher]
[13]. McDonagh E.M., Boukouvala S., Aklillu E., Hein D.W., Altman R.B., Klein T.E., PharmGKB summary: very important pharmacogene information for: N:-Acetyltransferase 2, *Pharmacogenetics and Genomics*, 2014, **24**:409 [Crossref], [Google Scholar], [Publisher]
[14]. Robinson P.K., Enzymes: principles and biotechnological applications, *Essays in Biochemistry*, 2015, **59**:1 [Crossref], [Google Scholar], [Publisher]
[15]. Rajasekaran M., Abirami S., Chen C., Effects of single nucleotide polymorphisms on human N-acetyltransferase 2 structure and dynamics by molecular dynamics simulation, *PloS one*, 2011, **6**:e25801 [Crossref], [Google Scholar], [Publisher]
[16]. Unissa A.N., Sukumar S., Hanna L.E., The role of N-Acetyl transferases on isoniazid resistance from mycobacterium tuberculosis and human: an in silico approach, *Tuberculosis and Respiratory Diseases*, 2017, **80**:255 [Crossref], [Google Scholar], [Publisher]

HOW TO CITE THIS ARTICLE
D.N. Rahardjo, Y.M. Mutiara, M. Wahjudi, R. Andrajati, R.A.D. Sartika, The Interaction of Isoniazid on 3D Structure Variation of NAT2 Gene and Its Effect on Drug Blood Levels. *J. Med. Chem. Sci*., 2024, 7(12) 1969-1981
DOI: https://doi.org/10.26655/JMCHEMSCI.2024.12.15
URL: https://www.jmchemsci.com/article_211333.html